

Electromagnetic Production of J/ψ at e^+e^- colliders and the Signature for Color-Octet

Chao-Hsi CHANG^{§,†}, Cong-Feng QIAO[§] and Jian-Xiong WANG^{§,‡}

[§] *CCAST (World Laboratory), P.O. Box 8730, Beijing 100080, China.**

[†] *Institute of Theoretical Physics, Academia Sinica, Beijing 100080, China.*

[‡] *Institute of High Energy Physics, Academia Sinica, Beijing 100039, China.*

Abstract

Electromagnetic production of J/ψ at e^+e^- colliders is investigated. It is expected to be as a further test of charmonium production of QED nature. We find that at the energies of CESR, BEPC, and TRISTAN (e.g. $4.0\text{GeV} \leq \sqrt{s} \leq 60\text{GeV}$), the contributions of the concerned electromagnetic processes to the J/ψ inclusive production are great, even dominant, thus they greatly effect the observation on the color-octet J/ψ production signature at e^+e^- colliders. The production of ψ' , being very similar to the one of J/ψ , is roughly estimated and its influence on the observation on the color-octet J/ψ production signature at e^+e^- collision is also discussed briefly.

PACS numbers: 12.20.Ds, 13.65.+i, 12.20.Fv, 12.38.Qk

Keywords: Electromagnetic Process, Charmonia Production, Color-singlet, Color-Octet, Electron Positron Annihilation

*Not mailing address for C.-H. CHANG and J.-X. WANG.

Corresponding author: Cong-Feng Qiao

E-mail: qcf@ccastb.ccast.ac.cn; Phone: 086-10-62568350; Fax: 086-10-62562586

Since J/ψ was discovered, its hadronic production has been an interesting problem so far, especially several important progresses have been achieved recently. The first is about the calculation of the fragmentation functions of a parton to double heavy mesons (heavy quarkonia and B_c meson etc.) and the study of the production mechanisms in perturbative QCD framework [1]. The second is about the comparison of the theoretical predictions, which are achieved due to the calculations of the fragmentation functions, with the experimental data of the J/ψ and ψ' prompt production [2]. As a result of the comparison, a disparity between the theoretical predictions and the Tevatron experimental data, the so-called ‘ $\psi'(\psi)$ plus’ puzzle, is found [3]. The third is very soon a plausible and interesting suggestion for solving the puzzle, the so-called ‘color-octet mechanism’, is put forward [4], and afterwards, the discussions about it and on it are spread broadly. To confirm the color-octet mechanisms further, several suggestions are proposed. Namely the investigations on all kinds of production mechanisms of the J/ψ production: the color singlet ones and the octet ones, at various energies and in various processes, not only at hadronic colliders but also at e^+e^- and ep colliders, have been carried out by groups [5–12]. Among them the J/ψ inclusive production in e^+e^- annihilation has been received special and wide attention, especially, since it was proposed to observe the color-octet signature through the inclusive J/ψ production in e^+e^- annihilation [11]. Being one of the best places to observe the color-octet signature because of its clean background, the J/ψ production in e^+e^- annihilation is emphasized by the authors [11–13]. Whereas, there are two kinds of J/ψ production in e^+e^- collision, i.e., i). the scattering production $e^+ + e^- \rightarrow e^+ + e^- + J/\psi$ (we will refer this production as scattering production later on in this paper) depicted as the Feynman diagrams Figs.1.a, 1.b. ii). the production associated with a hard photon $e^+ + e^- \rightarrow J/\psi + \gamma$ (we will refer this production as hard-photon production later on in this paper) depicted as Feynman diagrams Fig.1.c, which are less considered in literature. We are to investigate these two kinds of production mechanisms in this paper. Only very recently the hard-photon production $e^+e^- \rightarrow J/\psi + \gamma$ in the e^+e^- annihilation was computed by us and that process indeed has a great influence on the observation on the color-octet signature [14]. Nevertheless, we still think it is meaningful to consider those two kinds of J/ψ production (scattering and hard-photon production) together and to estimate their effects on the observation of the color-octet signature. Furthermore, there is another kind of J/ψ production: $e^+ + e^- \rightarrow J/\psi + f + \bar{f}$, where f, \bar{f} denote a pair of quark and anti-quark or lepton and anti-lepton, but not a pair of electron and positron. It is similar to the scattering production $e^+ + e^- \rightarrow e^+ + e^- + J/\psi$ at the

first glance, whereas in fact it, being always through e^+e^- s-channel annihilation, is much different from the scattering production. It suffers from the s-channel suppression due to the annihilation, especially with the collision energy increasing. Thus it is expected to be neither as great nor as important as the scattering one in effecting the observation of the color-octet signature. Therefore, We will not discuss this kind of production, $e^+ + e^- \rightarrow J/\psi + f + \bar{f}$, here, but leave it to a later detailed analysis [15].

Theoretically, from Figs.1.a-1.c it is easy to see that the processes are of QED nature. A common feature of them is that in corresponding diagram(s) there is always a virtual photon to couple to an electron line that plays a role similar to that in the J/ψ production in resonance in e^+e^- annihilation (or in the decay $J/\psi \rightarrow e^+e^-$). Thus, besides the factor, the processes are of pure QED. It is this reason that we will call the two kinds of production as electromagnetic production. To any given order in α , they may be computed reliably and precisely by means of calculating the corresponding Feynman diagrams. Note that for simplicity, only the typical Feynman diagram(s) for the electromagnetic J/ψ production is presented here. Of the scattering production $e^+e^- \rightarrow e^+e^- + J/\psi$ depicted as Fig.1.a and Fig.1.b, the diagram in Fig.1.b (and the other similar ones which are not shown) contains exchanges of a photon and an electron (or positron) in t-channel, thus the diagram is expected to contribute a dominant fraction to the cross section, especially, for the pieces of the phase-space, where the momenta of the exchanged photon and the electron are approaching to their mass shells, respectively. The hard-photon production, associated with a hard photon (the hard photon is emitted from the electron line, and the J/ψ couples to the electron line too, but indirectly through a virtual photon) depicted as Fig.1.c, is of order $O(\alpha^{\frac{3}{2}})$ in amplitude, i.e., one order lower in QED coupling constant than the scattering one. However, because it is an exchange electron (or positron) process in t-channel too, it is expected to make a great contribution in J/ψ production.

Because in the considered energy region here, comparatively rather ‘low’ energies are included, which may even comparable to $m_{J/\psi}$, the so-called electromagnetic fragmentation approach (EMFA) [5] is not applicable. The EMFA works well only at much high energies ($\sqrt{s} \gg m_{J/\psi}$). In addition, if one had adopted the electromagnetic fragmentation approach no matter how it had worked, there would be no advantages at all in the calculation of the processes. Hence to calculate the processes we will adopt a full QED approach rather than EMFA approach in this paper. For the hard-photon production if experimentally the hard photon can be observed, i.e. the process will be able to be measured exclusively, the process may be used as a test of the other QCD calculations even

calibrating the detector for experiments. For the production $e^+ + e^- \rightarrow e^+ + e^- + J/\psi$, besides the J/ψ connecting to all the possible ‘final’ or the ‘initial’ electron (positron) lines, the rest part of its corresponding Feynman diagrams is of pure QED, thus one may also calculate it reliably too, and if the e^+e^- pair maybe well detected experimentally, the process may also be used as another test of the QED calculation.

The electromagnetic production processes emphasized here are of a color-singlet production mechanism, nevertheless, they have contributions to the inclusive J/ψ production. Therefore, at various energies of present available collider facilities, such as TRISTAN, CESR and BEPC, to calculate the processes precisely are meaningful, especially, versus not only those of the other color-singlet production but also the color-octet production processes. It is certain that from the quantitative computation results the influences of the considered processes on the observation on the octet signature with inclusive J/ψ production in e^+e^- annihilation may exist to some degrees. In this paper we are to make the estimation and finally obtain an important conclusion. Because of the fact that i). there are more complications at relatively high energies, e.g. at $\sqrt{s} \geq m_Z$, the Z boson resonance effects will be brought about, and ii). the color-octet production, being a very interesting and a ‘s-channel’ process, is expected to be observable not at very high energies (at a very high energy, ‘s-channel’ processes will be suppressed strongly due to its s-channel propagator), in this paper we merely focus light on the relatively low energy region $\sqrt{s} \leq 60\text{GeV}$, which is related to the colliders TRISTAN, CESR and BEPC etc.. A more comprehensive study on J/ψ production at a more wider range of the energy will be presented elsewhere [15]. One will see below that the contribution from the scattering and hard-photon production process to inclusive J/ψ production in e^+e^- collision is substantial: the hard-photon one at comparatively low energies, but the scattering one at comparatively high energies.

Though theoretically and experimentally to study the J/ψ production in e^+e^- colliders has a quite long history, as pointed out above, yet the scattering production and the hard-photon one have not been well studied. As these two kinds of the production are of QED nature essentially (the former is described by the Feynman diagrams Figs.1.a-1.b, and the later by Fig. 1.c), the corresponding amplitude of each diagram may be written down immediately, and with straightforward calculations, the formulae for the differential cross sections may be obtained.

As the hard-photon production is relatively simple, its cross section may be written out analytically in a compact form. We will present the corresponding analytical formula

before doing numerical calculations. Whereas for the scattering production, it is a process of three-body final state, and it has more corresponding Feynman diagrams, thus it is much more complicated. It is hard to write the resultant formulae compactly in this letter, thus we will only present the numerical results for the scattering production here.

For the hard-photon production, finally the differential cross section can be expressed as:

$$\frac{d\sigma}{dt} = \frac{32\pi\alpha^3|R_S(0)|^2}{3M^3s^2} \left[\frac{2M^2s}{tu} + \frac{t}{u} + \frac{u}{t} \right], \quad (1)$$

here M is the charmonium mass; α is electromagnetic coupling constant;

$$s = (p_1 + p_2)^2; \quad t = (k - p_1)^2; \quad u = (P - p_1)^2.$$

We should note here that in eq.(1) the electron mass is ignored for shorten the representation, while in doing numerical calculations the mass will be kept. As the wave function at the origin $|R_S(0)|^2$ appearing here is exactly equal to that appearing in the corresponding equation for the decay $J/\psi \rightarrow e^+e^-$, i.e.

$$\Gamma(J/\psi \rightarrow e^+e^-) = \frac{4\alpha^2}{M^2}|R_S(0)|^2, \quad (2)$$

hence we will determine it from the experimental value of the width for the decay $J/\psi \rightarrow e^+e^-$. In this way, all of the theoretical corrections to the wave function at origin have been included because the two equations stand on the same foot theoretically. For the hard-photon production, the numerical values of the differential cross section versus t , hence the angular $\cos\theta$, at a given CMS energy and the total cross section versus the CMS energy now may be computed with the equation

$$\frac{d\sigma}{dt} = \frac{6\pi\alpha\Gamma^{exp.}(J/\psi \rightarrow e^+e^-)}{Ms^2} \left[\frac{2M^2s}{tu} + \frac{t}{u} + \frac{u}{t} \right], \quad (3)$$

or

$$\frac{d\sigma}{d\cos\theta} = \frac{6\pi\alpha\Gamma^{exp.}(J/\psi \rightarrow e^+e^-)s}{M(1-r)\sin^2\theta} [(1+r)^2 + (1-r)^2\cos^2\theta], \quad (4)$$

where $r \equiv M^2/s$. For the scattering production, it is easy to realize from the Feynman diagrams Fig.1.a and Fig.1.b that the cross section is also proportional to the wave function at the origin $|R_S(0)|^2$. In the numerical calculations, we input the value of the wave function at the origin as the same way as that in the hard-photon production.

The total cross sections for various kinds of the production by e^+e^- collision are plotted in Fig.2. As pointed out above, we are interested in seeing the influences of the hard-photon and the scattering production on the observation of the color octet signature through observing the inclusive J/ψ production, thus in Fig.2 the color-octet one depicted as Feynman diagram Fig.1.d and a color-singlet one as Feynman diagram Fig.1.e are selected for a precise comparison. The production depicted as the Feynman diagrams Fig.1.d and that by Fig.1.e have been studied, and their details in calculations may be found in literatures [12,13]. So as we do the numerical computations, instead of re-computing them from the very beginning we adopt the relevant formulae from the original papers directly: those for the color-octet ones from [8], and those for the color-singlet one from [12].

In fact, as discussed above for the scattering production, the relevant Feynman diagrams may be divided into two sub-groups: one always contains an e^+e^- annihilation (Fig.1.a) and the other always contains a ‘t-channel’ exchange of a photon (Fig.1.b). For the reason that the process contains a photon exchanges in t-channel in its Feynman diagrams, we call this process as scattering production and the sub-group shown as Fig.1.b as a ‘scattering group’ in this paper. It is easy to check that each group itself is gauge invariant. To see the contribution from each group, in Fig.3 we plot the contributions not only from each sub-group, but the whole contribution from the both groups as well, although there is interference between the two groups when calculating the cross section of the scattering production. Indeed from Fig.3 one may see that the scattering sub-group contributes dominantly over the other one. For the same reason, the scattering production becomes the greatest among the various kinds of production at high energies (Fig.2), although in the amplitude it is at least one order higher in $\alpha^{\frac{1}{2}}$ than most of the others. The similar production $e^+e^- \rightarrow J/\psi + f\bar{f}$ ($f \neq e$), as discussed before, containing the Feynman diagrams as Fig.1.a only, is expected to be smaller and not so important as the scattering one in inclusive J/ψ production in e^+e^- annihilation, so we will not discuss them here.

For the production: the scattering one (Figs.1.a-1.b), the hard-photon one (Fig.1.c), the color-octet one (Fig.1.d), and the color-singlet one (Fig.1.e), the differential cross sections $d\sigma/d\cos\theta$ versus $\cos\theta$, which denotes the angle between the directions of the produced J/ψ and the colliding beam, are plotted in Figs.4.a-4.c. The CMS energies are taken at where the colliders BEPC, CESR and TRISTAN have accumulated quite a lot of data, respectively. In order to see the behavior of the dependence of the differential

cross section of the scattering J/ψ production on the energy more precisely, we plot the curves for the differential cross section at several energies together in Fig.5. Now, from Figs.4.a-4.c and Fig.5 as well, one may see the features of different J/ψ production process in angular distribution quite well.

In fact, a complete set of the Feynman diagram always contains a Z boson exchange one in replacing of the virtual photon in each diagram of Figs.1.a-1.e. Whereas at low energies, $\sqrt{s} \leq m_Z$, such as those at BEPC and CESR even TRISTON, all the contributions from the Z boson exchange diagrams are small, thus they may be negligible in the case. At high energies, equal or higher than that of LEP-I, the virtual Z boson may approach to its mass shell, and the contribution from the Z boson exchange may become great. Therefore we cannot ignore them without a careful checking. Indeed, the effects from the Feynman diagrams like Fig.1.a but with the virtual photon from the e^+e^- annihilation replaced by a Z boson make a peak around the Z resonance for the the relevant curves in Fig.3. In general at such a high energy, more complications and more kinds of production processes will be brought in, thus at present moment we would restrain ourselves to discuss the relative low energy situation only, but postpone the discussions for high energies ($\sqrt{s} \geq m_Z$) elsewhere [15].

From Fig.2, one can see that the contribution from the scattering production at comparatively high energies and from the hard-photon production at comparatively low energies are dominant among all kinds of the considered production processes. Furthermore from Figs.4.a-4.c one may see the fact that the electromagnetic production has a common feature: the differential cross section of the production approaches to the maximum when the produced J/ψ approaches to the beam direction, but it is still significant at large P_T for the produced J/ψ . It is due to both of them being dominated by ‘t-channel’ exchange diagrams. The hard-photon and scattering J/ψ production (the former in the comparatively low energies, but the later in the comparatively high energies) in the direction perpendicular to that of the beams still contribute such a fraction, not much smaller than the greatest one among the considered ‘others’, although the greatest one among the considered ‘others’ is alternated when the CMS energy is increasing. For instance, the color-singlet one corresponding to the Feynman diagram Fig.1.e is smaller than those of the color-octet ones to the Feynman diagram Fig.1.d in the energy region $\sqrt{s} \leq 12\text{GeV}$, while the situation is changed totally in the energy region $\sqrt{s} \geq 12\text{GeV}$. Moreover we should note here that *the hard-photon and the scattering production have a similar angular distribution in shape as those of the color-octet production* and the shape is emphasize

as the signature of the color octet production by the authors [11].

In showing the energy dependence, i.e. the total cross sections versus the CMS energies for various kinds of production, considering the fact that it is impossible to measure either the hard photon or the pair of e^+e^- experimentally if the photon or the e^+e^- pair goes out close enough to the beam direction, we have plotted two curves in Fig.2 for each of them: one with a cut on the outgoing angular of J/ψ and the other without any cut. From Fig.2 one may easily see the difference without a cut and with a cut $20^\circ \leq \theta \leq 160^\circ$ on the angular between the beam direction and that of the produced J/ψ .

For ψ' production, in fact, anyone of the mechanisms will act the same as it does for J/ψ , because ψ' , being a radial excited state of J/ψ , just has the same quantum numbers. Moreover the electromagnetic production of J/ψ has a common feature, i.e. the J/ψ always couples to a charged fermion line through a virtual photon. Thus, we must have a very similar result for the electromagnetic production of ψ' . The reason is that the electromagnetic ψ' production has just the same Feynman diagrams as Figs.1.a-1.c, but the leg for J/ψ is replaced by that for ψ' . Hence the difference between the electromagnetic production of these two particles is only due to the wave function at origin and the slight different masses. It is well known that the squared absolute values of the wave function at origin of J/ψ and ψ' respectively are different roughly by a factor 2, i.e. the one for J/ψ is about two times large than that of for ψ' . And both of the two particles are on mass-shell in the production, the effect due to the mass difference $\Delta m \equiv m_{\psi'} - m_{J/\psi}$ can be only within $\leq 4\%$ if the true value of the mass difference is considered. Hence, in fact, the electromagnetic ψ' production is roughly equal to one half of that of the electromagnetic J/ψ production. As the branching ratio of the decay $\psi' \rightarrow J/\psi + \dots$ is quite great $\sim 57\%$, in e^+e^- collision the signal of the ψ' production with a prompt cascade decay to J/ψ may generate an event pattern, which looks like as that of the direct color-octet J/ψ production or of the direct color-singlet J/ψ production very much. Thus, the ψ' production will also disturb the signature of the color-octet J/ψ production at certain level.

We should note here that in the figures the input values of the color-octet matrix elements for the color-octet production are taken from the determination [8] by fitting the Tevatron data [2]. As they are not consistent with other determinations based on different measurements and the ref. [8] values seem overestimated, the estimations here for the color-octet production are probably also overestimated.

In conclusion, the electromagnetic production (the hard-photon production and the

scattering production) in e^+e^- collision itself is interesting because it has been less considered so far. It has a different feature from the ‘others’ depicted as Feynman diagrams Figs.1.d and Figs.1.e, because it is dominated by ‘t-channel’ exchange mainly but not as the ‘others’ through ‘s-channel’ annihilation only. We would like to emphasize once more here that for the hard-photon production, if experimentally the hard photon can be identified well, i.e. the process will be measured exclusively, we may use the experimental measurements to test the calculation which is mainly based on QED. Even the process may be used in calibrating the detector for relevant experiments. In addition, if experimentally the e^+e^- pair besides the J/ψ from the process $e^+ + e^- \rightarrow e^+ + e^- + J/\psi$ may be observed exclusively, the process may also be used as one more test of the calculation. As for the ψ' production, the situation is more complicated, we will not discuss here but in [15]. If one would like, as suggested by [11], to observe the signature of the color-octet mechanism in e^+e^- annihilation merely through the inclusive J/ψ production at comparative low energies of the presented colliders, such as those of BEPC, CESR and TRIESTON, one has to take into account the contribution of the electromagnetic production not only for J/ψ but also for ψ' carefully, that is emphasized specially in this paper. One should precisely take away that sources as the background of the color-octet signature from the inclusive production in advance. In principle, it may be practicable by precise exclusive measurements of the J/ψ production as much as possible. e.g. not only to measure the produced J/ψ but also to tag the associated hard photon for the hard-photon J/ψ production or to tag the e^+e^- pair for the scattering J/ψ production precisely and to distinguish the ψ' production with a cascade decay to J/ψ from the direct production etc..

Acknowledgements

This work was supported in part by the National Science Foundation of China, the Grant LWTZ-1298 of the Chinese Academy of Sciences, and the Postdoctoral Science Foundation of China.

REFERENCES

- [1] C.-H. Chang, Y.-Q. Chen, *Phys. Lett.* **B284** (1992) 127; *Phys. Rev.* **D46** (1992) 3845; *ibid* **D50** (1994) 6013(E); E. Braaten, T.C. Yuan, *Phys. Rev. Lett.* **71** (1993) 1673; E. Braaten, K. Cheung, T.C. Yuan, *Phys. Rev.* **D48** (1993) 4230; *ibid* R5049 ; V.V. Kiselev, A.K. Likhoded, M.V. Shevlyagin, *Z. Phys. C* **63** (1994) 77; Y.-Q. Chen, *Phys. Rev.* **D48** (1993) 5181; *ibid* **D50** (1994) 6013(E);
- [2] F. Abe *et al.* (CDF collaboration), *Phys. Rev. Lett.* **69** (1992) 3704; *ibid* **71** (1993) 2537.
- [3] M. Doncheski, S. Fleming, M.L. Mangano, *Proceedings of the Workshop on Physics at Current Accelerators and Supercolliders* Ed. J.L. Hewett, A.R. White, D. Zeppenfeld; E. Braaten, M.A. Doncheski, S. Fleming, M.L. Mangano, *Phys. Lett.* **333** (1994) 548; M. Cacciari, M. Greco, *Phys. Rev. Lett.* **73** (1994) 1586.
- [4] E. Braaten, S. Fleming, *Phys. Rev. Lett.* **74** (1995) 3327.
- [5] S. Fleming, *Phys. Rev.* **D50** (1994) 5808.
- [6] V.M. Driesen, J.H. Kühn, E. Mirkes, *Phys. Rev.* **D49** (1994) 3197;
- [7] P. Ko, J. Lee, H.S. Song, *Phys. Rev.* **D54** (1996) 4312.
- [8] P. Cho, A.K. Leibovich, *Phys. Rev.* **D53** (1996) 150; *ibid* **D53** (1996) 6203.
- [9] K. Cheung, W.-Y. Keung, T.C. Yuan, *ibid* **76** (1996) 877.
- [10] M. Beneke, I. Z. Rothstein, *Phys. Rev.* **D54** (1996) 2205.
- [11] E. Braaten, Y.-Q. Chen, *Phys. Rev. Lett.* **76** (1996) 730.
- [12] P. Cho, A. K. Leibovich, *Phys. Rev.* **D54** (1996) 6690.
- [13] F. Yuan, C.-F. Qiao, K.-T. Chao, *Phys. Rev.* **D56**, (1997) 321.
- [14] C.-H. Chang, C.-F. Qiao, J.-X. Wang, to appear in *Phys. Rev.* **D**.
- [15] C.-H. Chang, C.-F. Qiao, J.-X. Wang, in preparation.

FIGURE CAPTIONS

Fig.1:

Fig.1.a. Typical Feynman diagram for the production of $e^+e^- \rightarrow e^+ + e^- + J/\psi$ via e^+e^- ‘annihilation’.

Fig.1.b. Typical Feynman diagram for the production of $e^+e^- \rightarrow e^+e^- + J/\psi$ via ‘scattering’ (a photon and an electron exchange in t-channel).

Fig.1.c. Typical Feynman diagram for the production of $e^+e^- \rightarrow \gamma + J/\psi$ via e^+e^- ‘annihilation’ and an electron exchange in t-channel.

Fig.1.d. Some typical color-octet Feynman diagrams for the production of $e^+e^- \rightarrow g + J/\psi$ via e^+e^- ‘annihilation’.

Fig.1.e. Typical color-singlet Feynman diagram for the production of $e^+e^- \rightarrow g + g + J/\psi$ via e^+e^- ‘annihilation’.

Fig.2. The total cross sections of the production J/ψ versus the CMS energy \sqrt{s} for the various mechanisms: the thin solid curve presents that for the hard-photon production without cut; but the thick solid one presents that with a cut $20^\circ \leq \theta \leq 160^\circ$; the thin dashed curve presents the scattering production without cut; but the thick dashed one presents that with a cut $20^\circ \leq \theta \leq 160^\circ$; the thin dotted one presents that for the color-octet mechanism $e^+e^- \rightarrow g + {}^1S_0[8]$; the thick dotted one presents that for the color-octet mechanism $e^+e^- \rightarrow g + {}^3P_J[8]$; the dashed-dotted one presents that for the color-singlet mechanism $e^+e^- \rightarrow g + g + J/\psi$.

Fig.3 The total cross sections for the production $e^+e^- \rightarrow e^+ + e^- + J/\psi$: the thin solid line presents the total cross section; the dashed-dotted one presents that with a cut $20^\circ \leq \theta \leq 160^\circ$; the dashed one presents the contribution only from Feynman diagrams Fig.1a; the dotted one presents the contribution only from Feynman diagrams Fig.1b.

Fig.4:

Fig.4.a. For the various mechanisms at the CMS energy $\sqrt{s} = 4.03\text{GeV}$ (BEPC), the differential cross sections $d\sigma/d\cos\theta$ of the J/ψ production versus $\cos\theta$. The thin solid curve presents that for the hard-photon production; The thick solid curve presents that for the scattering production; the dashed one presents that for the color-octet production $e^+e^- \rightarrow g + {}^1S_0[8]$; the dotted one presents that for the color-octet production $e^+e^- \rightarrow g + {}^3P_J[8]$; the dashed-dotted one presents that for the color-singlet production.

Fig.4.b. The same as those of Fig.4.a but at the CMS energy $\sqrt{s} = 10.6\text{GeV}$ (CESR).

The types of the curves have the same meaning.

Fig.4.c. The same as those of Fig.4.a but at the CMS energy $\sqrt{s} = 64.0\text{GeV}$ (TRISTAN).

The types of the curves have the same meaning.

Fig.5 The differential cross sections $d\sigma/d\cos\theta$ of the electromagnetic J/ψ production versus $\cos\theta$ at various CMS energies.

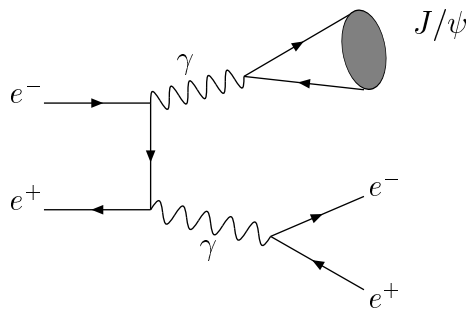


Fig.1.a

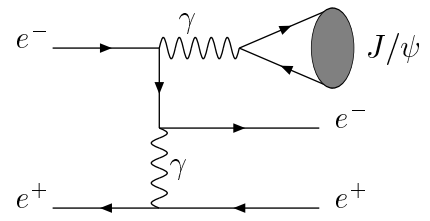


Fig.1.b

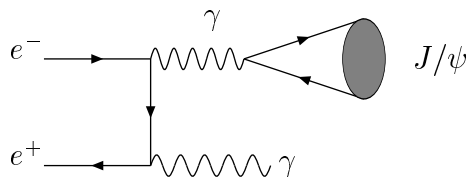


Fig.1.c

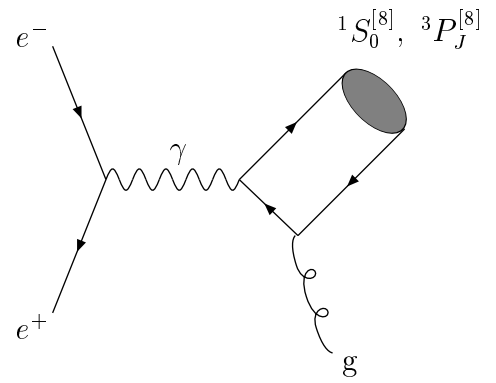


Fig.1.d

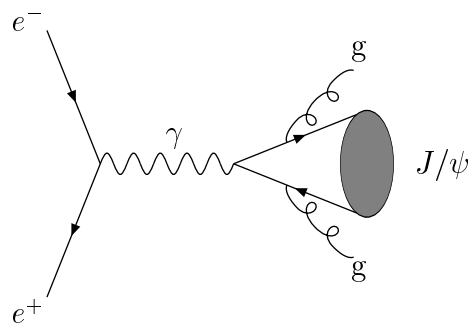


Fig.1.e

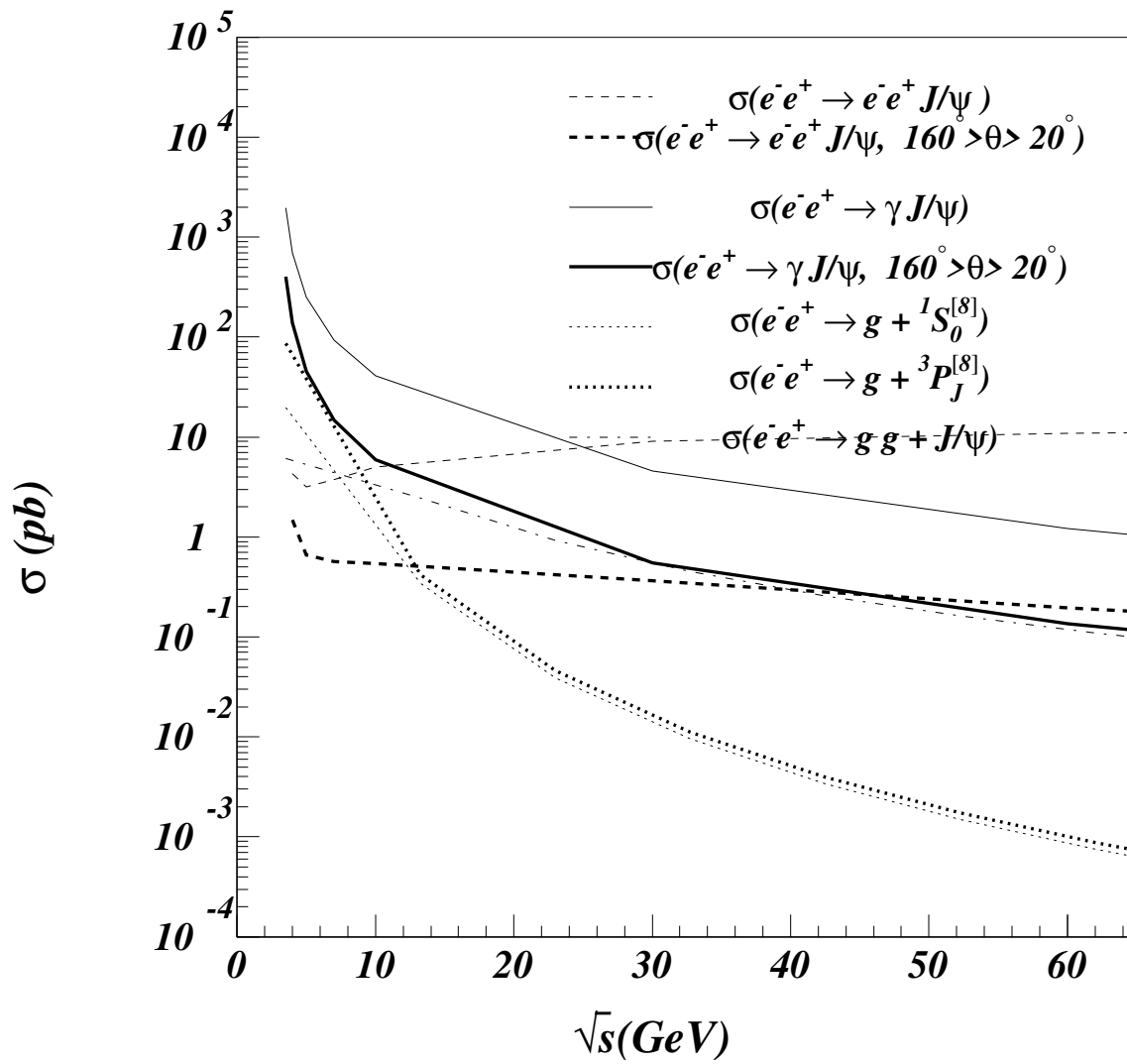


Fig. 2

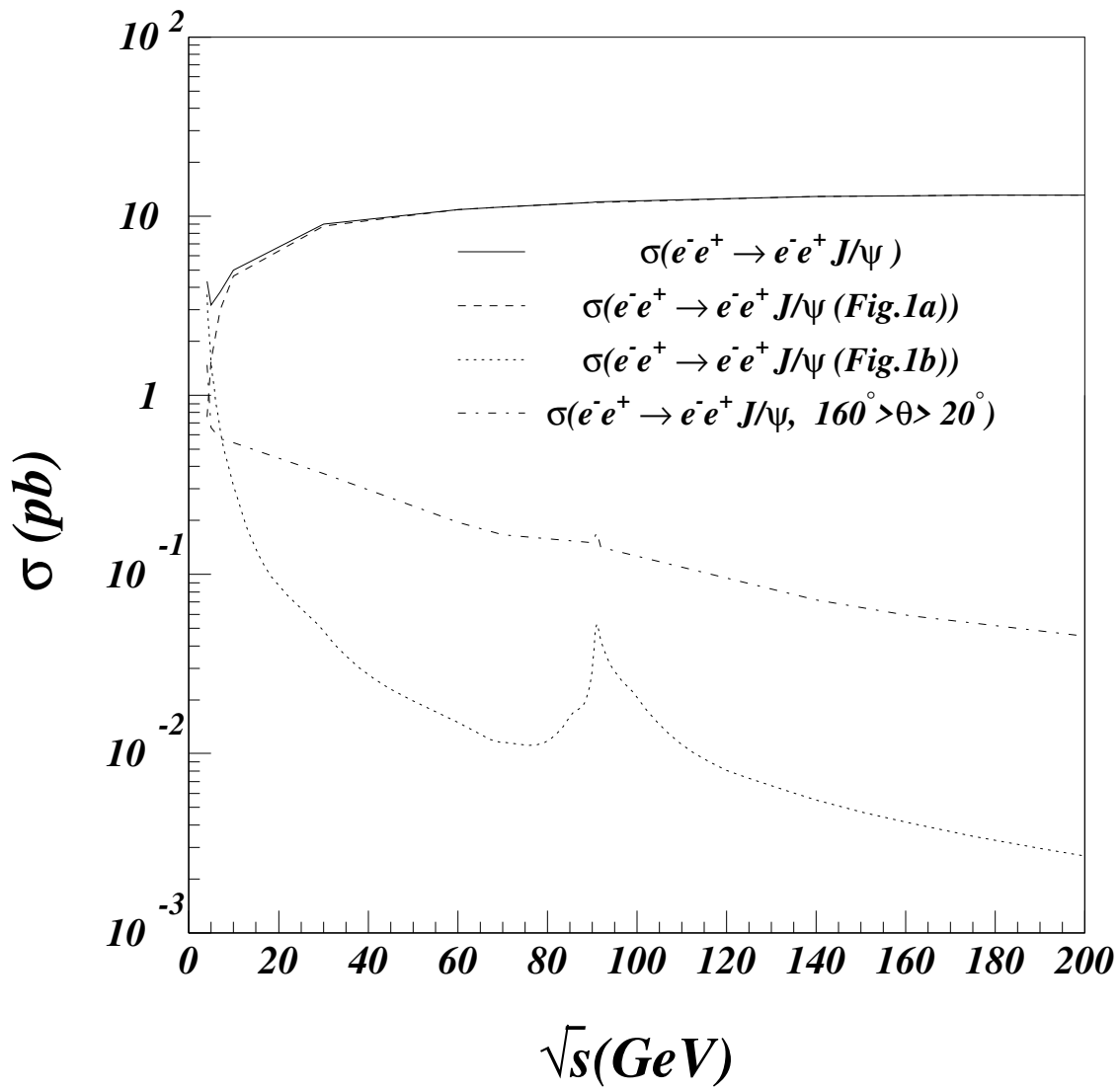


Fig. 3

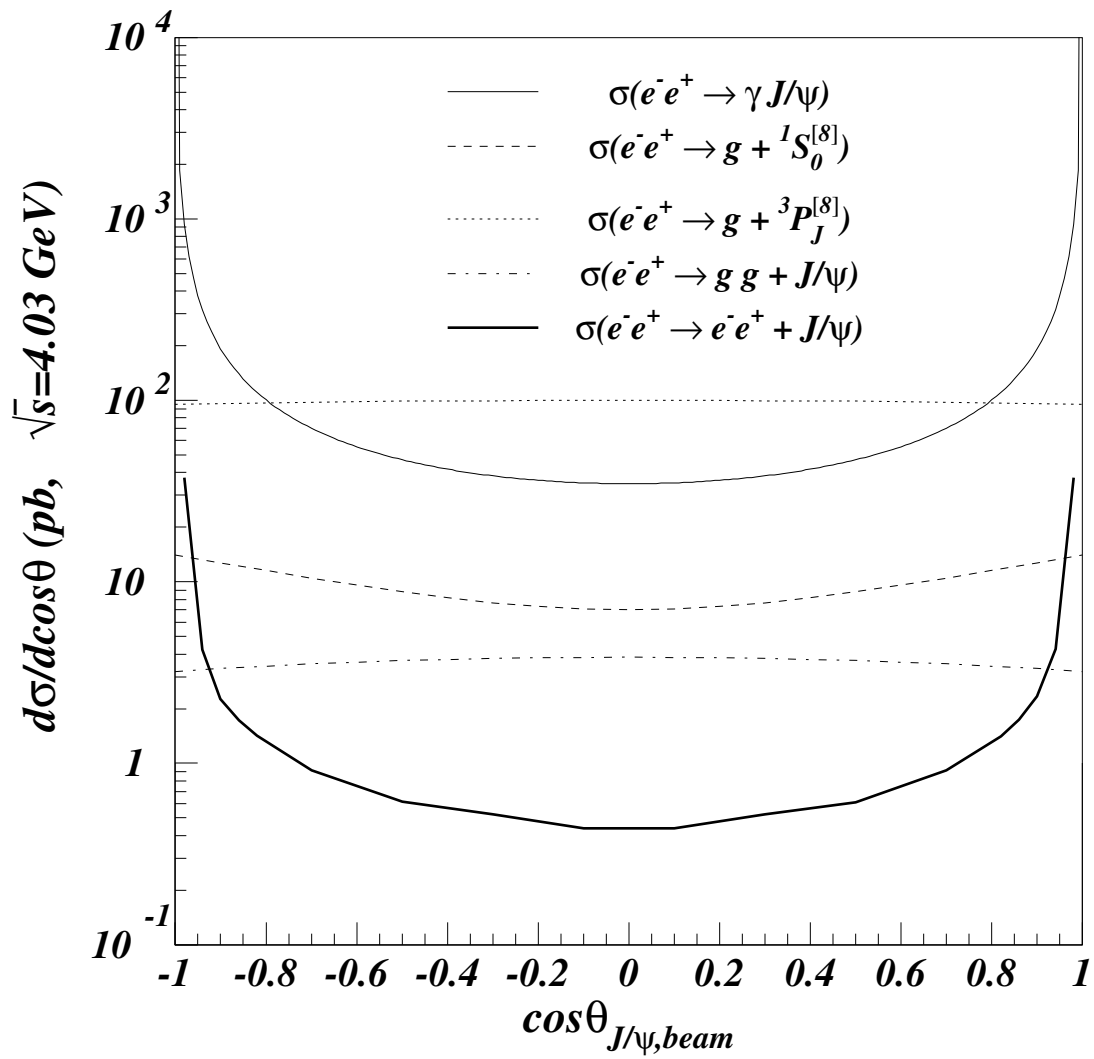


Fig.4.a

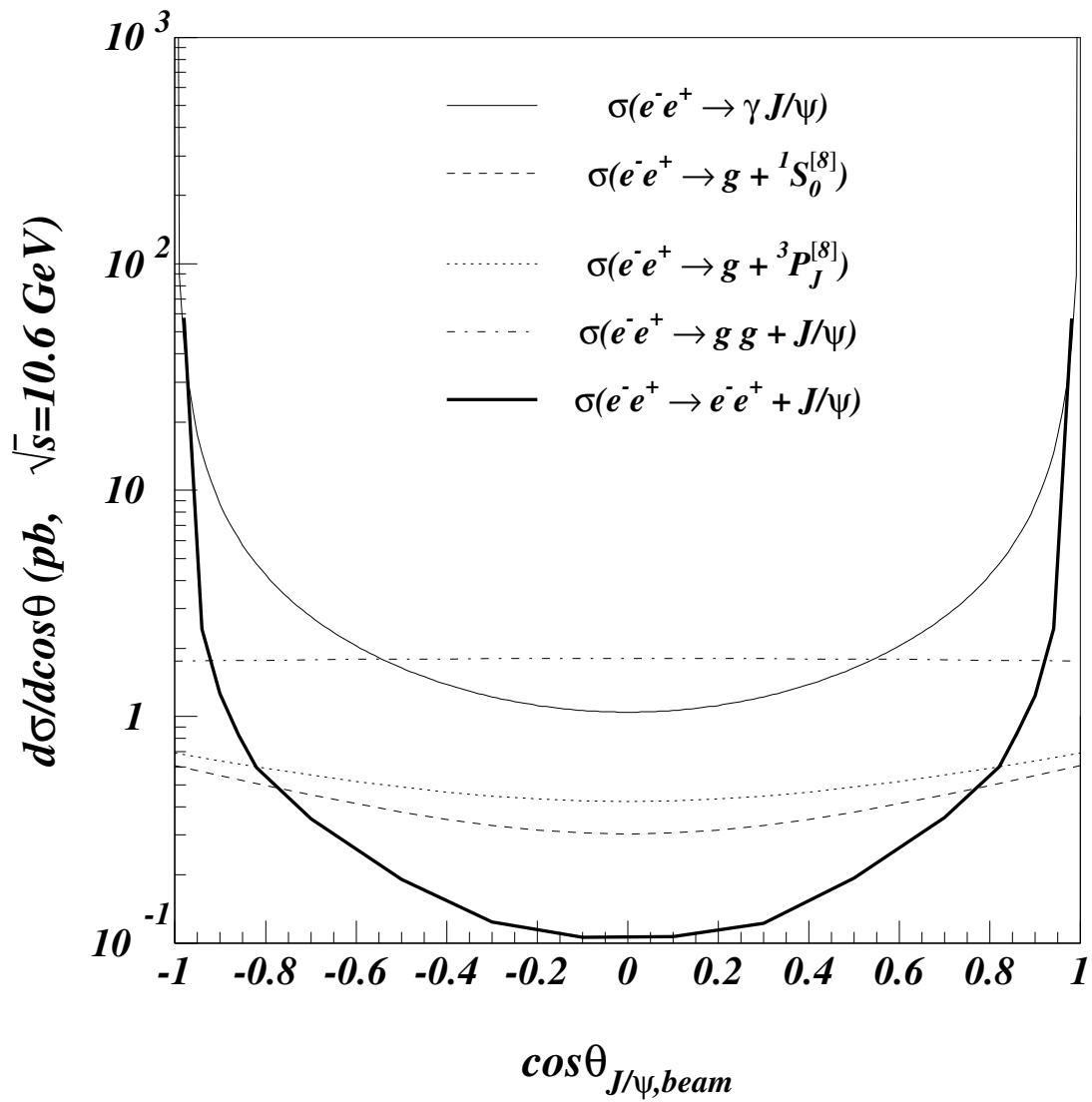


Fig.4.b

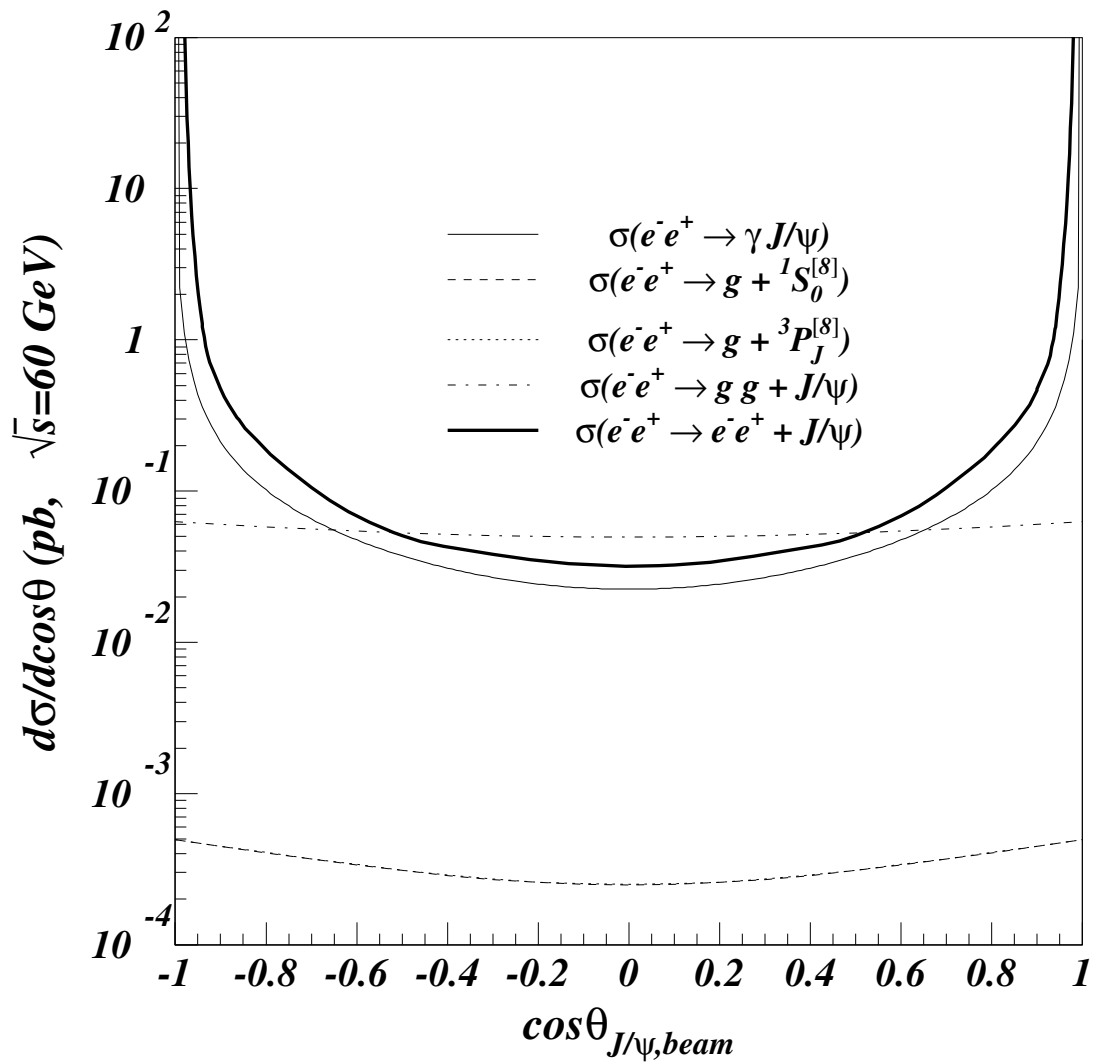


Fig. 4.c

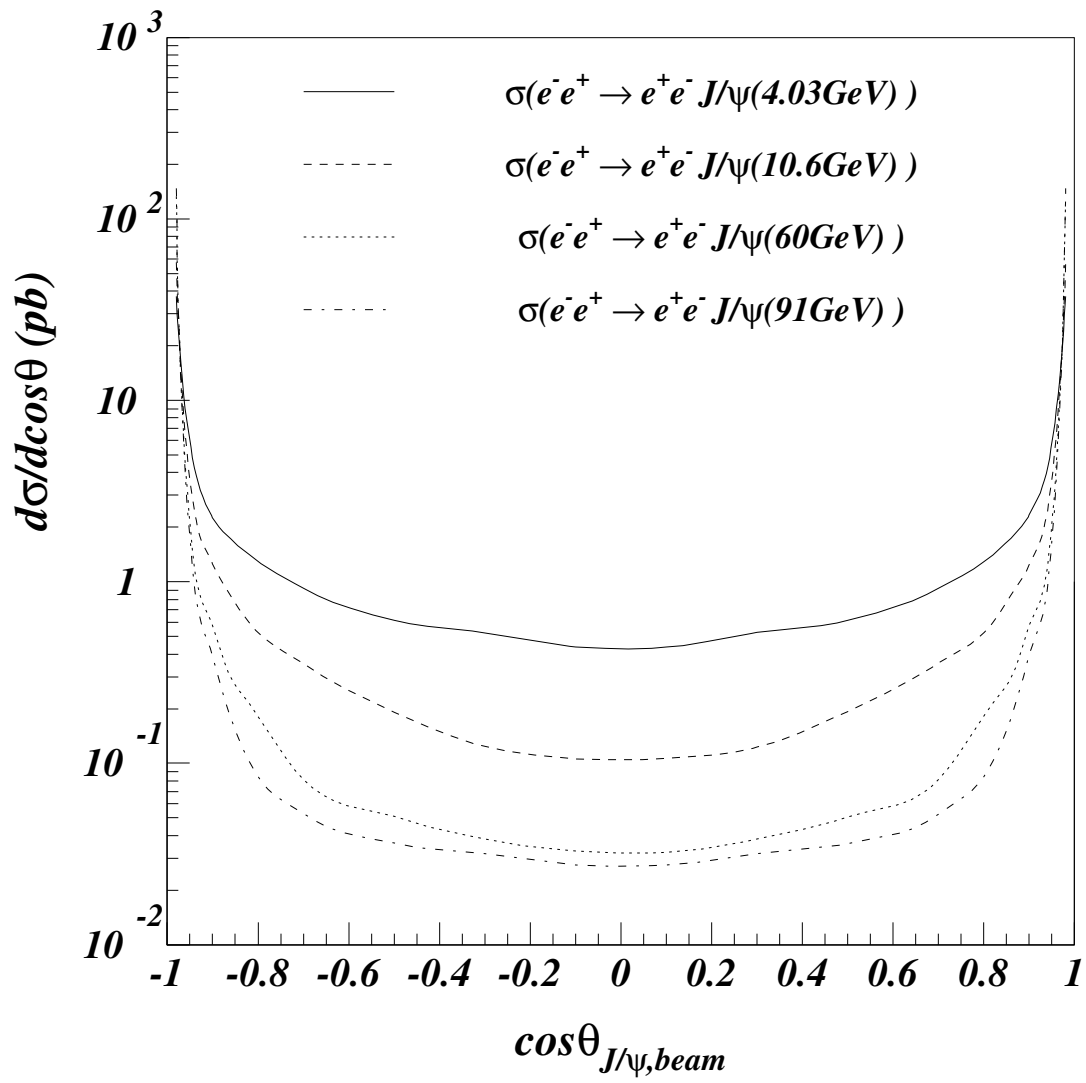


Fig.5